11

Ferroelectrics Study at Microwaves

Yuriy Poplavko, Yuriy Prokopenko,
Vitaliy Molchanov and Victor Kazmirenko
National Technical University "Kiev Polytechnic Institute"
Ukraine

1. Introduction

Dielectric materials are of interest for various fields of microwave engineering. They are widely investigated for numerous applications in electronic components such as dielectric resonators, dielectric substrates, decoupling capacitors, absorbent materials, phase shifters, etc. Electric polarization and loss of dielectric materials are important topics of solid state physics as well. Understanding their nature requires accurate measurement of main dielectric characteristics. Ferroelectrics constitute important class of dielectric materials. Microwave study of ferroelectrics is required not only because of their applications, but also because important physical properties of theses materials, such as phase transitions, are observed at microwave frequencies. Furthermore, most of ferroelectrics have polydomain structure and domain walls resonant (or relaxation) frequency is located in the microwave range. Lattice dynamics theory also predicts strong anomalies in ferroelectric properties just at microwaves. That is why microwave study can support the investigation of many fundamental characteristics of ferroelectrics.

Dielectric properties of materials are observed in their interaction with electromagnetic field. Fundamental ability of dielectric materials to increase stored charge of the capacitor was used for years and still used to measure permittivity and loss at relatively low frequencies, up to about 1 MHz (Gevorgian & Kollberg, 2001). At microwaves studied material is usually placed inside transmission line, such as coaxial or rectangular waveguide, or resonant cavity and its influence onto wave propagation conditions is used to estimate specimen's properties. Distinct feature of ferroelectric and related materials is their high dielectric constant ($\varepsilon = 10^2 - 10^4$) and sometimes large dielectric loss ($\tan\delta = 0.01 - 1$). High loss could make resonant curve too fuzzy or dissipate most part incident electromagnetic energy, so reflected or transmitted part becomes hard to register. Also because of high permittivity most part of incident energy may just reflect from sample's surface. So generally conventional methods of dielectrics study may not work well, and special approaches required.

Another problem is ferroelectric films investigation. Non-linear ferroelectric films are perspective for monolithic microwave integrated circuits (MMIC) where they are applied as linear and nonlinear capacitors (Vendik, 1979), microwave tunable resonant filters (Vendik et al., 1999), integrated microwave phase shifter (Erker et al., 2000), etc. Proper design of these devices requires reliable evidence of film microwave dielectric constant and loss tangent. Ferroelectric solid solution $(Ba,Sr)TiO_3$ (BST) is the most studied material for

possible microwave applications. Lucky for microwave applications, BST film dielectric constant in comparison with bulk ceramics decreases about 10 times (ε_{film} ~ 400 – 1000) that is important for device matching. Temperature dependence of ε_{film} becomes slick that provides device thermal stability (Vendik, 1979), and loss remains within reasonable limits: tanδ ~ 0.01 – 0.05 (Vendik et al., 1999). Accurate and reliable measurement of ferroelectric films dielectric properties is an actual problem not only of electronic industry but for material science as well. Film-to-bulk ability comparison is an interesting problem in physics of ferroelectrics. Properties transformation in thin film could be either favourable or an adverse factor for electronic devices. Ferroelectric materials are highly sensitive to any influence. While deposited thin film must adapt itself to the substrate that has quite different thermal and mechanical properties. Most of widely used techniques require deposition of electrodes system to form interdigital capacitor or planar waveguide. That introduces additional influence and natural film's properties remain unknown.
Therefore, accurate and reliable measuring of dielectric constant and loss factor of bulk and thin film ferroelectrics and related materials remains an actual problem of material science as well as electronic industry.

2. Bulk ferroelectrics study

At present time, microwave study of dielectrics with ε of about 2 – 100 and low loss is well developed. Some of theses techniques can be applied to study materials with higher permittivity. Approximate classification of most widely used methods for large-ε materials microwave study is shown in Fig. 1.

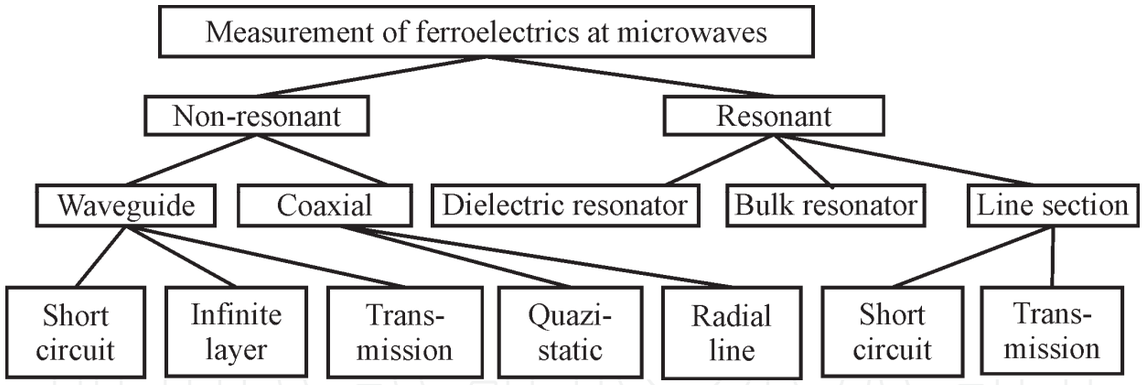

Fig. 1. Microwave methods for ferroelectrics study

Because of high dielectric constant, microwave measuring of ferroelectrics is quite unconventional. The major problem of high-ε dielectric microwave study is a poor interaction of electromagnetic wave with studied specimen. Because of significant difference in the wave impedance, most part of electromagnetic energy reflects from air-dielectric boundary and can not penetrate the specimen. That is why, short-circuited waveguide method exhibit lack of sensitivity. If the loss of dielectric is also big, the sample of a few millimetres length looks like "endless". For the same reason, in the transmission experiment, only a small part of electromagnetic energy passes through the sample to output that is not sufficient for network analyzer accurate operation. Opened microwave systems such as resonators or microstrip line suffer from approximations.

One of the most used methods utilizes measurement cell in the form of coaxial line section. Studied specimen is located in the discontinuity of central line. Electric field within the specimen is almost uniform only for materials with relatively low permittivity. This is quazistatic approximation that makes calculation formulas simpler. If quazistatic conditions could not be met, then radial line has to be studied without approximations. For the high ε materials coaxial method has limitations. Firstly, samples in form of thin disk have to be machined with high precision in a form of disk or cylinder. Secondly, many ferroelectric materials have anisotropic properties, so electric field distribution in the coaxial line is not suitable. This work indicates that a rectangular waveguide can be improved for ferroelectrics study at microwaves.

2.1 Improved waveguide method of ferroelectrics measurements

The obvious solution to improve accuracy of measurement is to reinforce interaction of electromagnetic field with the material under study. One of possible ways is to use dielectric transformer that decreases reflection. For microwave study, high-ε samples are placed in the cross-section of rectangular waveguide together with dielectric transformers, as shown in Fig. 2.

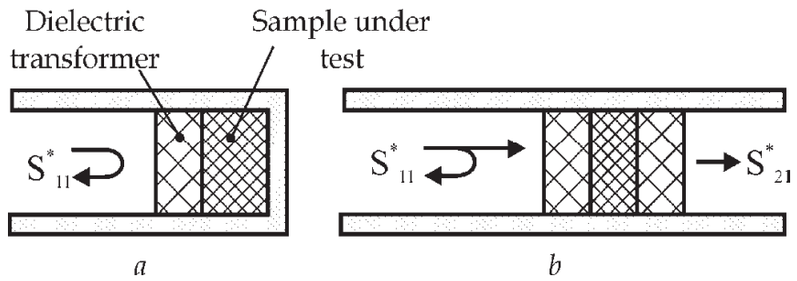

Fig. 2. Measurement scheme: *a*) short-circuit line method, *b*) transmission/reflection method

A quarter-wave dielectric transformer with $\varepsilon_{trans} = \sqrt{\varepsilon_{sample}}$ can provide a perfect matching, but at one certain frequency only. In this case, the simple formulas for dielectric constant and loss calculations can be drawn. However, mentioned requirement is difficult to implement. Foremost, studied material dielectric constant is unknown *a priori* while transformer with a suitable dielectric constant is also rarely available. Secondly, the critical limitation is method validity for only one fixed frequency, for which transformer length is equal precisely to quarter of the wavelength. Moreover, the calculation formulas derived with the assumption of quarter wave length transformers lose their accuracy, as last requirement is not perfectly met.

Insertion of dielectric transformers still may improve matching of studied specimen with air filled part of waveguide, though its length and/or permittivity do not deliver perfectly quarter wave length at the frequency of measurement. Dielectric transformers with ε_{trans} = 2 – 10 of around quarter-wave thickness are most suitable for this purpose. Influence of transformers must be accurately accounted in calculations.

2.2 Method description

The air filled section of waveguide, the transformer, and the studied sample are represented by normalized transmission matrices $\tilde{\mathbf{T}}$, which are the functions of lengths and

electromagnetic properties of neighbour areas. Applying boundary conditions normalized transmission matrix for the basic mode can be expressed as:

$$\tilde{\mathbf{T}}_i = \sqrt{\frac{\mu_{i-1}}{\mu_i}} \cdot \begin{bmatrix} \frac{\gamma_i + \gamma_{i-1}}{2\sqrt{\gamma_{i-1}\gamma_i}} e^{-j\dot{\gamma}_i d} & \frac{\gamma_i - \gamma_{i-1}}{2\sqrt{\gamma_{i-1}\gamma_i}} e^{-j\dot{\gamma}_i d} \\ \frac{\gamma_i - \gamma_{i-1}}{2\sqrt{\gamma_{i-1}\gamma_i}} e^{j\dot{\gamma}_i d} & \frac{\gamma_i + \gamma_{i-1}}{2\sqrt{\gamma_{i-1}\gamma_i}} e^{j\dot{\gamma}_i d} \end{bmatrix}, \tag{1}$$

where μ_i is permeability of i-th medium; γ_i is propagation constant in i-th medium; d is the length of i-th medium. Transmission matrix of whole network can be obtained by the multiplication of each area transmission matrices:

$$[\tilde{\mathbf{T}}] = \tilde{\mathbf{T}}_n \cdot \tilde{\mathbf{T}}_{n-1} \cdot \ldots \cdot \tilde{\mathbf{T}}_1 . \tag{2}$$

The order of multiplying here is such, that matrix of the first medium on the wave's way appears rightmost. Then, for the convenience, the network transmission matrices can be converted into scattering matrices whose parameters are measured directly.

In case of non-magnetic materials scattering equations, derived from (2), can be solved for every given frequency. However, this point-by-point technique is strongly affected by accidental errors and individual initiations of high-order modes. To reduce influence of these errors in modern techniques vector network analyzer is used to record frequency dependence of scattering parameters (Baker-Jarvis, 1990). Special data processing procedure, which is resistive to the individual errors, such as nonlinear least-squares curve fitting should be used:

$$\min_{(\varepsilon', \varepsilon'')} \sum_n \sigma_n \left(S_n^{meas} - S(f_n, \varepsilon', \varepsilon'') \right)^2 . \tag{3}$$

Here σ_n is the weight function; S_n^{meas} is measured S-parameter at frequency f_n; $S(f_n, \varepsilon', \varepsilon'')$ is calculated value of scattering parameter at the same frequency, assuming tested material to have parameters ε' and ε''. Real and imaginary parts of scattering parameters are separated numerically and treated as an independent, i.e. the fitting is applied to both real and imaginary parts.

Proper choice of weight is important for correct data processing. Among possible ways, there are weighted derivatives, and the modulus of reflection or transmission coefficients. These methods emphasize the influence of points near the minimum values of the reflection or transmission, which just exactly have the highest sensitivity to properties of studied material.

The choice between short-circuited line or transmission/ reflection methods depends on which method has better sensitivity, and should be applied individually.

2.3 Examples of measurements

Three common and easily available materials were used for experimental study. Samples were prepared in the rectangular shape that is adjusted to *X*-band waveguide cross section. Side edges of samples for all experiments were covered by silver paste. Summary on measured values is presented in Table 1.

Material	Reflection		Transmission	
	ε	tanδ	ε	tanδ
TiO_2	96	0.01	95	0.01
$SrTiO_3$	290	0.02	270	0.017
$BaTiO_3$	590	0.3		

Table 1. Summary on several studied ferroelectric materials

Measured data and processing curves are illustrated in Fig. 3, 4. In reflection experiment minima of S_{11} are deep enough to perform their reliable measurement, so numerical model coincides well with experimentally acquired points. For transmission experiment total amount of energy passed trough sample is relatively low, but there are distinct maxima of transmission, which also are registered reliably.

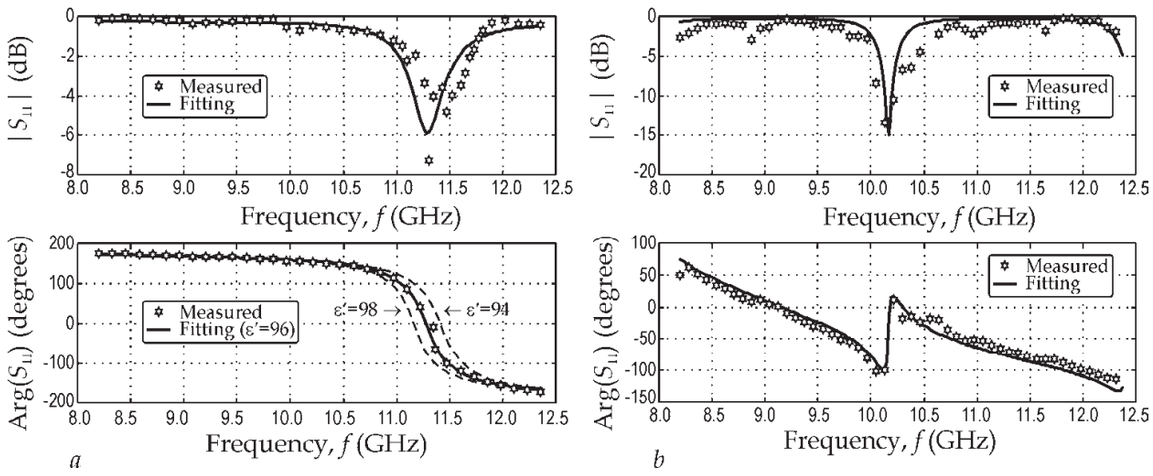

Fig. 3. Measured data and processing for reflection experiments: TiO_2, ε = 96, thickness 2.03 mm (*a*); $SrTiO_3$ of 3.89 mm thickness with 6.56 mm teflon transformer (*b*)

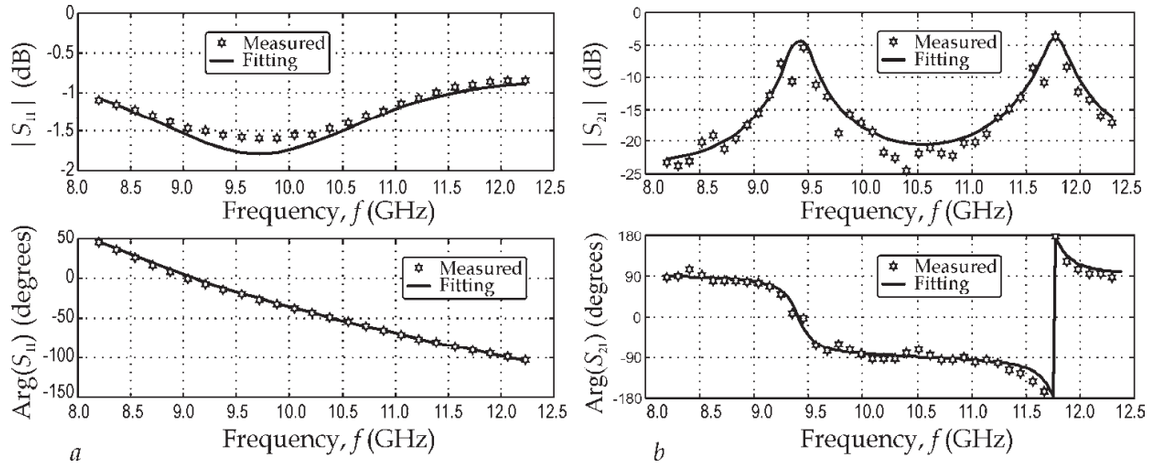

Fig. 4. Measured data and processing for: 1.51mm $BaTiO_3$ with 6.56 mm teflon transformer (*a*), reflection experiment; 3.89 mm $SrTiO_3$, transmission experiment (*b*)

$BaTiO_3$ is very lossy material with high permittivity. In reflection experiment, Fig. 4, there is fuzzy minimum of S_{11}, so calculation of permittivity with resonant techniques is inaccurate. Change in reflection coefficient across whole X-band is about 0.5 dB, so loss determination by resonant technique might be inaccurate too. Our calculations using fitting procedure (3) show good agreement with other studies in literature.

2.4 Order-disorder type ferroelectrics at microwaves

There are two main frequency intervals of dielectric permittivity dispersion: domain walls relaxation in the polar phase and dipole relations in all phases. Rochelle Salt is typical example of this behaviour, Fig. 5. Here and after ε_1, ε_2, ε_3 are diagonal components of permittivity tensor.

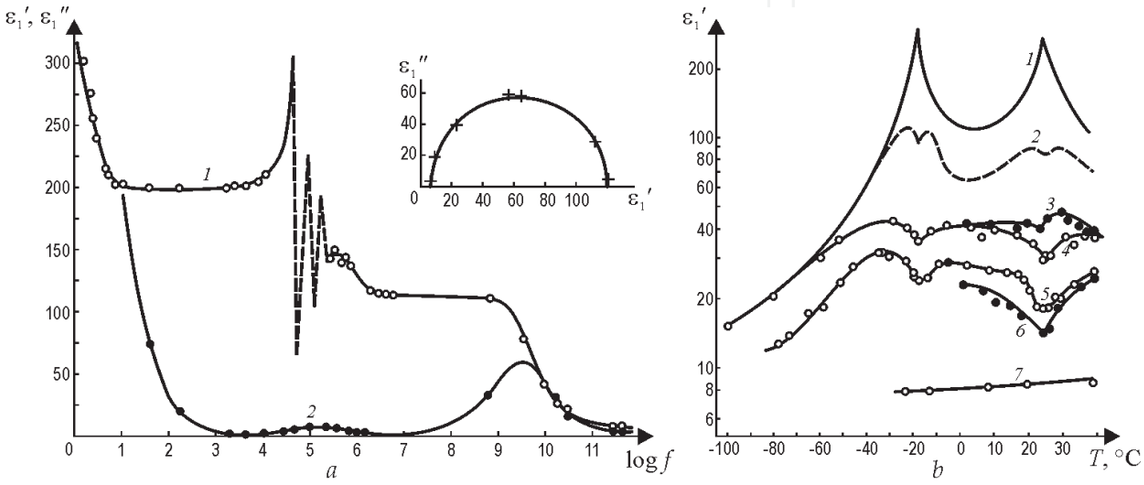

Fig. 5. Rochelle Salt microwave study: ε'_1 and ε''_1 frequency dependence at 18° C (*a*); ε'_1 temperature dependence at frequencies (in GHz): *1* – 0.8; *2* – 5.1; *3* – 8.4; *4* – 10.2; *5* – 20.5; *6* – 27; *7* – 250 (*b*)

Sharp maxima of at $\varepsilon'_1(f)$ in the frequency interval of 10^4 – 10^5 Hz mean piezoelectric resonances that is accompanied by a fluent ε'-decrease near 10^6 Hz, Fig. 5, *a*. The last is domain relaxation that follows electromechanical resonances. In the microwaves Rochelle Salt ε'_1 dispersion with ε''_1 broad maximum characterizes dipole relaxation that can be described by Debye equation

$$\varepsilon^*(\omega) = \varepsilon_\infty + \frac{\varepsilon(0) - \varepsilon(\infty)}{1 + i\omega\tau}, \tag{4}$$

where τ is relaxation time, $\varepsilon(\infty)$ is infrared and optical input to ε_1 why $\varepsilon(0)$ is dielectric permittivity before microwave dispersion started.

Microwave dispersion in the Rochelle Salt is observed in all phases (in the paraelectric phase above 24°C, in the ferroelectric phase between –18° – +24°C, and in the antiferroelectric phase below –18°C, Fig. 5, *b*. To describe $\varepsilon^*(\omega,T)$ dependence in all these phases using eq. (1) one need substitute in the paraelectric phase $\tau = \tau_0/(T - \theta)$ and $\varepsilon(0) - \varepsilon(\infty) = C/(T - \theta)$. Experiment shows that in paraelectric phase C = 1700 K, θ = 291 K and $\tau_0 = 3.2 \cdot 10^{-10}$ s/K. By the analogy this calculations can be done in all phases of Rochelle Salt.

Figure 6 shows main results of microwave study of TGS (another well known order-disorder type ferroelectric). Dipole relaxation in the polar phase demonstrates $\varepsilon'_2(f)$ decrease between 10 and 300 GHz with $\varepsilon''_2(f)$ maximum near 100 GHz, Fig. 6, *a*. Note, that 1 cm^{-1} corresponds to f = 30 GHz.

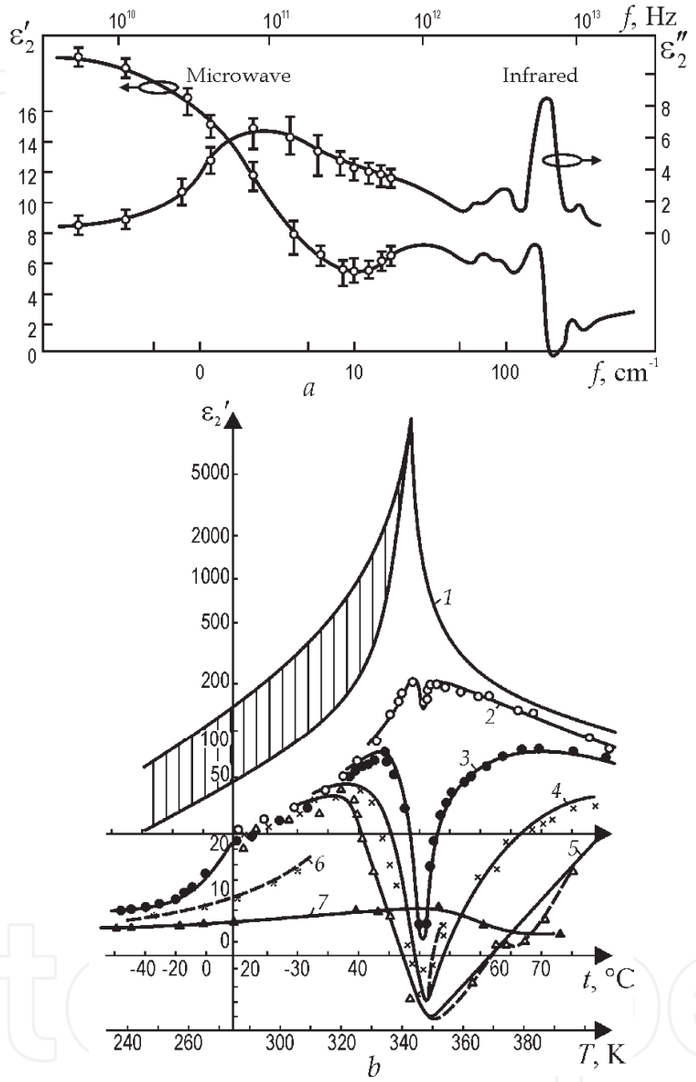

Fig. 6. TGS crystals microwave study: ε'_2 and ε''_2 frequency dependence at 300 K (*a*); ε'_2 temperature dependence at frequencies: *1* – 1 KHz, *2* – GHz, *3* – 16 GHz, *4* – 26 GHz, *5* – 37 GHz , *6* – 80 GHz, *7*– 250 GHz (*b*)

In contrast to Rochelle Salt, TGS is not piezoelectric in the paraelectric phase. In the Curie point $\varepsilon'_2(T)$ at microwaves demonstrates minimum. The family of $\varepsilon^*_2(f,T)$ characteristics can be well described by the modified Debye equation

$$\varepsilon^*(\omega,T) = \varepsilon_{IR} + \frac{C}{T-\theta+i\omega\tau_0} \tag{5}$$

where ε_{IR} is the infrared input to permittivity. In a paraelectric phase TGS crystal microwave properties can be described by the parameters C = 3200 K, θ = 321 K and $\tau_0 = 2 \cdot 10^{-10}$ sec/K. Microwave properties of the DKDP $\varepsilon^*_3(f, T)$ dependences that is characterized by the heavy deuteron relaxation looks very similar to TGS and Rochelle Salt crystals, Fig. 7, *a*. However, in the KDP crystals protons dynamics makes dielectric dispersion spectra similar to displace ferroelectric, Fig. 7, *b*.

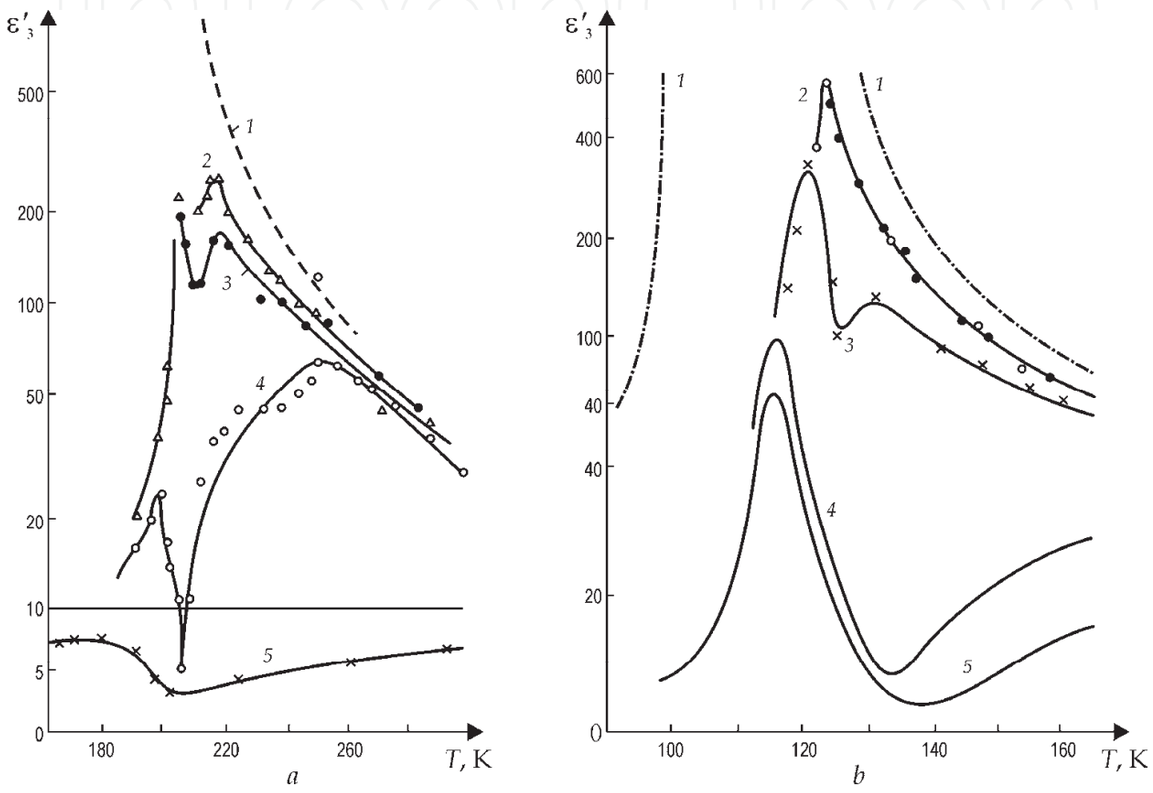

Fig. 7. Microwave dielectric dispersion in ferroelectrics of KDP type: KD_2PO_4 $\varepsilon'_3(T)$ at frequencies: 1 – 0.3 GHz; *2* – 8.6 GHz ; *3* – 9.7 GHz ; 4 – 26 GHz; 5 – 250 GHz (*a*); KH_2PO_4 $\varepsilon'_3(T)$ at frequencies: *1* – 1 kHz, *2* –9.4 GHz; *3* – 80 GHz , *4* –200 GHz; *5* –340 GHz (*b*)

2.5 Ferroelectrics of displace type at microwaves

In the ferroelectric phase the ε-dispersion at microwaves depends on domain walls vibration. That is why in the single-domain crystal practically no decrease in ε at microwaves is observed, as it is shown in Fig. 8, *a* with the example of $LiNbO_3$ crystal. Resonant change in ε_3 and ε_1 at megahertz frequencies means only piezoelectric resonances while far infrared ε-maxima are obliged to the lattice vibrations.

However, in the multidomain crystals dielectric dispersion at microwaves results in ε-decrease that is accompanied by tanδ maximum near frequency 9 GHz, shown in Fig. 8, *b* for multidomain $LiTaO_3$ crystal (there are also many piezoelectric resonances in the megahertz area).

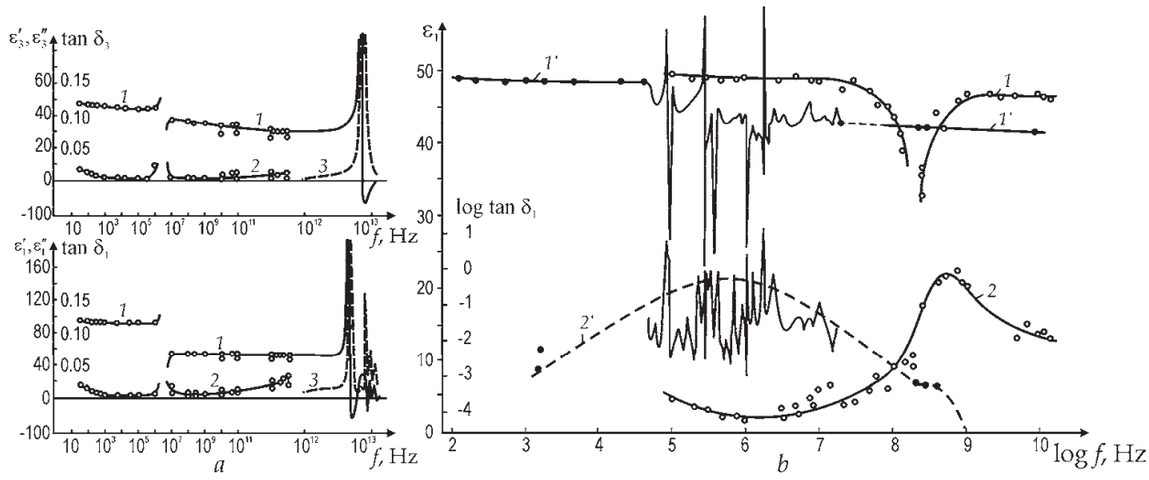

Fig. 8. Dielectric spectrums of ferroelectric crystals at 300 K: single domain $LiNbO_3$ ε_3 and $\tan\delta_3$, ε_1 and $\tan\delta_1$ (*a*); $LiTaO_3$: *1* - ε_1, *2* – $\tan\delta_1$ single domain; *1* – ε_1, *2* – $\tan\delta_1$ for multidomain crystal (*b*)

Polycrystalline ferroelectrics have obviously multidomain structure and, as a result, show microwave ε-dispersion, as it is shown in Fig. 9 for $PbTiO_3$ and $BaTiO_3$ (ε″ maximum is observed near frequency of 9 GHz while ε′ decreases in two times). More "soft" ceramics $Ba(Ti,Sn)O_3$ demonstrate microwave dispersion at lower but microwave frequencies: broad ε″ maximum is seen at 1 GHz.

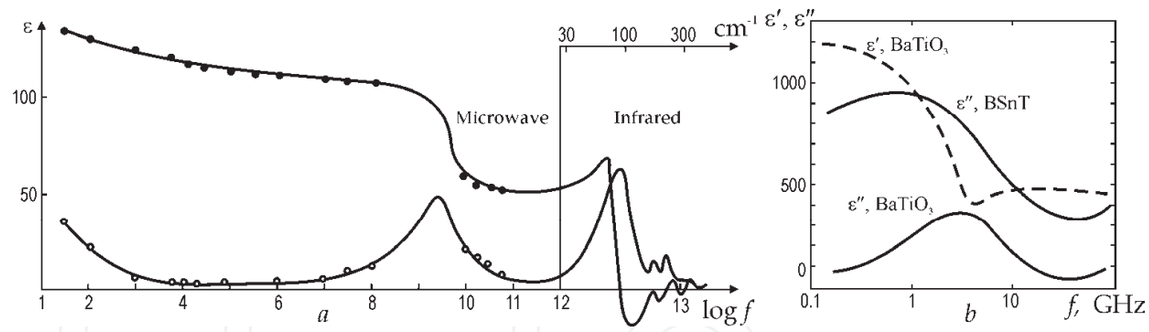

Fig. 9. Ferroelectric permittivity frequency dependence at 300 K: $PbTiO_3$ ceramics 1 - ε′ and 2 - ε″ (*a*); ceramics $BaTiO_3$ and $Ba(Ti,Sn)O_3$ = BSnT microwave study (*b*)

Microwave properties of displace type ferroelectrics in the paraelectric phase depends on soft lattice vibration mode. That is why Lorentz oscillator model is a basic model to describe ε* frequency dependence:

$$\varepsilon^*(\omega) = \varepsilon_\infty + \frac{\varepsilon(0) - \varepsilon(\infty)}{1 + (\omega/\omega_{TO})^2 + i\Gamma\omega/\omega_{TO}}. \tag{6}$$

In this equation let assume $\varepsilon(0) - \varepsilon(\infty) = C/(T-\theta)$ and soft mode critical frequency dependence on temperature is $\omega_{TO} = A\sqrt{T-\theta}$. Relative damping factor is $\Gamma = \gamma/\omega_{TO}$, as a result:

$$\varepsilon'(\omega,T)-\varepsilon_\infty = CA^2\frac{A^2(T-\theta)-\omega^2}{\left[A^2(T-\theta)-\omega^2\right]^2+\gamma^2\omega^2};$$

$$\varepsilon''(\omega,T)-\varepsilon_\infty = CA^2\frac{\gamma\omega}{\left[A^2(T-\theta)-\omega^2\right]^2+\gamma^2\omega^2}; \qquad (7)$$

$$\operatorname{tg}\delta \approx \frac{\gamma\omega}{A^2(T-\theta)},$$

where A is Cochran coefficient, C is Curie-Weiss constant, γ is damping coefficient. From ε and tanδ temperature dependences at various frequencies, as for instance Fig. 10, *a*, soft mode temperature dependence can be calculated, Fig. 10, *b*. Main lattice dynamics parameters of studied ferroelectrics are shown in Table 2.

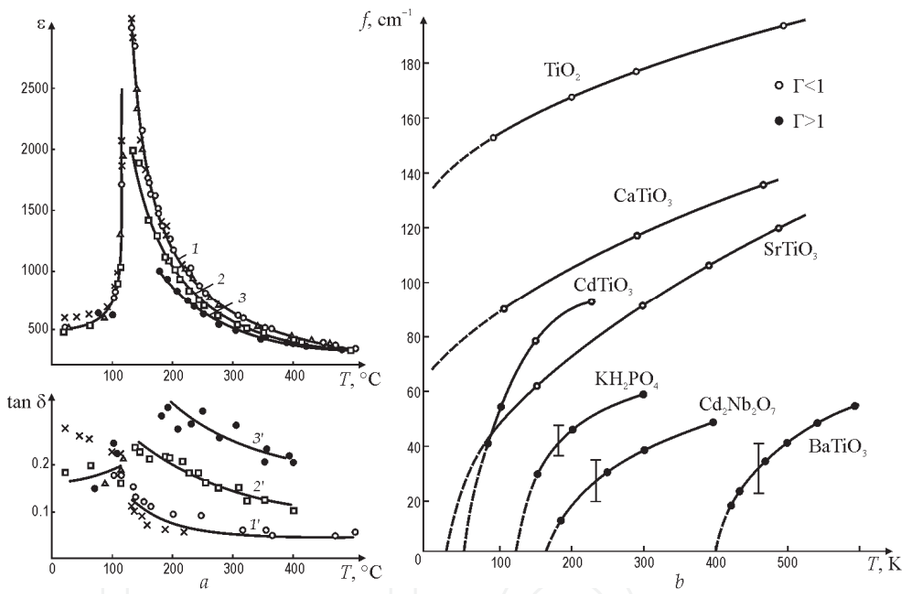

Fig.10. Paraelectrics at microwaves: $BaTiO_3$ ε (*1, 2, 3*) and tanδ (*1′, 2′, 3′*) temperature dependence at different frequencies: *1* – 9.4–37 GHz; *2* – 46 GHz; *3* – 76 GHz (*a*); soft modes frequency dependence for various paraelectrics obtained by microwave and far infrared experiments (*b*)

Material	P_c, μQ/cm²	$T_к$, K	θ, K	$C\cdot10^{-4}$, K	A/2π, GHz · $K^{-1/2}$
$CaTiO_3$	–	–	– 90	4.5	170
$SrTiO_3$	–	–	35	8.4	180
$BaTiO_3$	30	400	388	12	75
$PbTiO_3$	80	780	730	15	90
$KNbO_3$	30	685	625	18	95
$LiNbO_3$	70	1500	–	–	–

Table 2. Lattice parameters of some ferroelectric materials

3. Ferroelectric films investigation

3.1 Various methods comparison

Most of existing studies of ferroelectric films (22 published experiments listed in the review by Gevorgian & Kollberg, 2001) are drawn with the use of electrodes. For instance, the opposite-electrodes method is employed to study the system Pt/BST/Pt (Banieki et al., 1998). However, in most cases, ferroelectric film is studied between planar electrodes applied to the opened surface of the film. In that case, film parameters can be extracted from the impedance of interdigital planar capacitor as well as from the coplanar phase shifter study. Nevertheless, in all mentioned methods, the "natural film" microwave ε and tanδ remain unknown, because a complex system of "electrode-film-electrode" is investigated. Nevertheless, the data related to the "natural film" as well as to film components properties and substrates properties are important: their frequency and temperature characteristics are shown in Fig. 11.

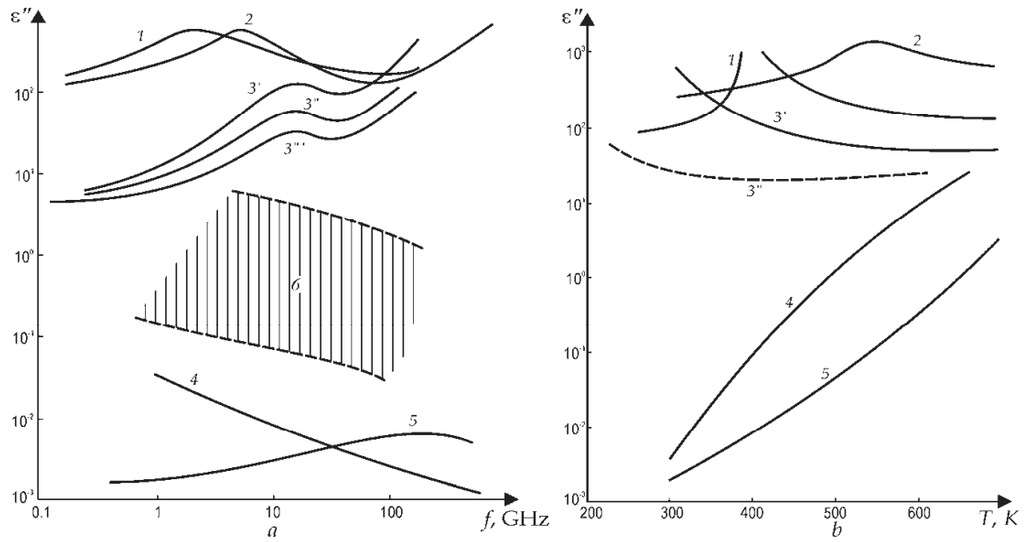

Fig. 11. Films, ceramics and crystals characterization at microwaves; ε″frequency dependence at 300 K: *1* – $BaTiO_3$ ceramics; *2* – $PbTi,ZrO_3$ ceramics; *3′*– BST ($Ba,SrTiO_3$) ceramics; *3″*– BST film 15 μm, 3‴ – BST film 2 μm, *4* – Si crystal, *5* – GaAs crystal; 6 – mixed oxides of BaO, TiO_2, PbO, SrO before film synthesis (*a*); ε″ temperature dependence at 80 GHz: *1* – $BaTiO_3$ ceramics; *2* –$PbTi,ZrO_3$ ceramics, *3′*– BST ceramics, *3″*– BST film 15 μm, *4* – Si crystal, *5* – GaAs crystal (*b*)

It is necessary to note that dielectric constant calculation from the planar capacitance is approximate while microwave loss cannot be even estimated. Point is that metallic electrodes strongly affect onto measured ε_{film} value (and especially onto film's tanδ) through the mechanical stress and skin effect in electrodes. Moreover, as a rule, dielectric parameters of film with interdigital electrodes are usually obtained at low frequency (of about 1 MHz); however, next this information is applied to microwave device elaboration. In the mass production small portion of the substrate could be sacrificed for test electrodes area. However, in laboratory study, single film gets unusable after electrodes deposition. So the electrodeless techniques are very important. A comparison of different methods of ferroelectric film study at microwaves is shown in Fig. 12.

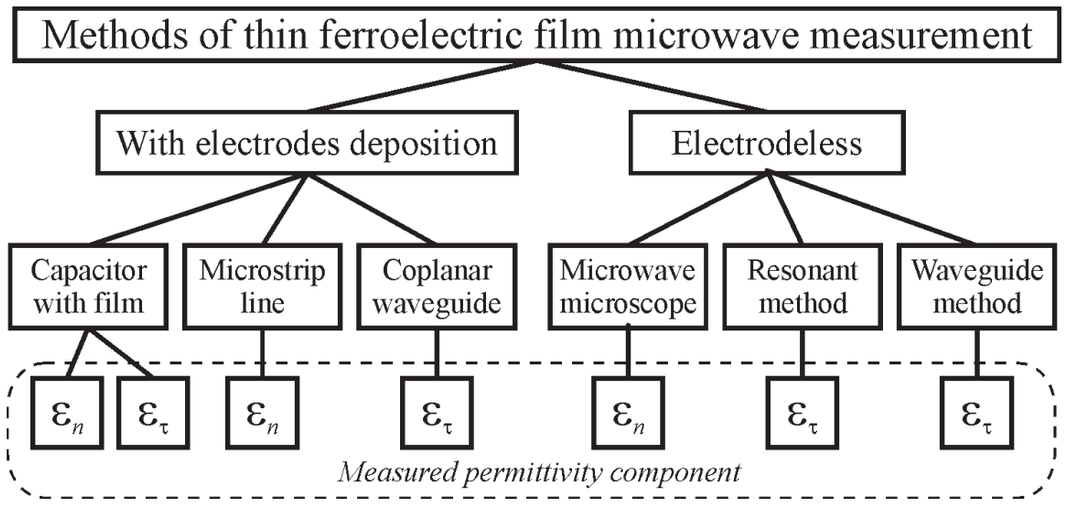

Fig. 12. Microwave methods for ferroelectric films study

Thin ferroelectric film is usually deposited onto dielectric substrate. Practically used films have thickness of 0.1–1 mm. Thermal expansion coefficient and lattice parameter of the substrate are different from those of thin film. Thus, film suffers from mechanical stress. This stress changes films properties comparing to the properties of bulk ferroelectric. Dielectric constant and loss could be decreased by order of magnitude. On the other hand, directional mechanical stress contributes to the anisotropy of film's parameters. So methods of films study must not only register film's response, but consider anisotropy as well.
Because of high dielectric constant and loss microwave testing of ferroelectrics is quite complex. In thin film study a question becomes even more complicated by film small thickness. This work presents waveguide method, suitable for thin films study.

3.2 Waveguide method description

Common technique for dielectric material measuring in the waveguide usually relies on complex scattering parameters measurement of waveguide section which cross section is filled with studied material. That technique can be easily adapted for measurement of the layered structures where properties of one layer are unknown.
However, this approach faces irresolvable difficulties with thin films. Simple estimation shows that X-band waveguide being entirely baffled with film of 1 μm thickness that has $\varepsilon = 1000$ and $\tan\delta = 0.05$ has phase perturbation of only about 0.4°, and brings attenuation of about -0.002 dB. These quantities are obviously out of equipment resolution capabilities. That is why, the goal is to arrange the interaction of film with electromagnetic field in such a way that brings recognizable response.
In proposed method, film-on-substrate specimen is centrally situated along the waveguide (Fig. 13). It is known that electric field intensity is highest in centre of waveguide so highest possible interaction of film with the electric field is provided.
Dielectric constant and loss can be found by solving scattering equations at one certain frequency. However, the accuracy of one-point technique is strongly affected by the accidental error (Baker-Jarvis, 1990). Proposed method accuracy is improved by the recording of complete frequency dependence of scattering parameters using contemporary vector network analyzer. Similarly to the method for bulk samples study, gathered experimental data then processed utilizing nonlinear least squares curve fitting technique (3).

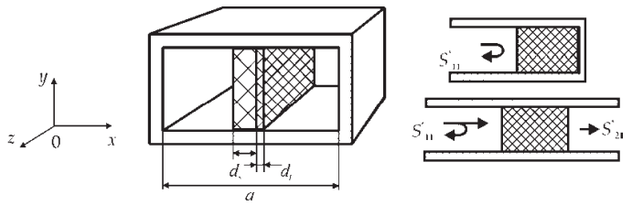

Fig. 13. Schematic representation of experiment

For the *S*-parameters calculations, electromagnetic field problem can be solved utilizing longitudinal wave representation (Egorov, 1967), (Balanis, 1989). Applying boundary conditions on media boundaries yields a complex nonlinear equation with respect to complex propagation constant:

$$\begin{aligned}
&\beta_s \tan\left(\beta_s \frac{a}{2} - \varphi_s\right) = \beta_f \tan\left(\beta_f \frac{a}{2} - \varphi_f\right);\\
&\varphi_s = \beta_s\left(\frac{a}{2} - d_s\right) + \operatorname{atan}\left[\frac{\beta}{\beta_s}\cot\left(\beta\left(\frac{a}{2} - d_s\right)\right)\right];\\
&\varphi_f = \beta_f\left(\frac{a}{2} + d_f\right) + \operatorname{atan}\left[\frac{\beta}{\beta_f}\cot\left(\beta\left(\frac{a}{2} + d_f\right)\right)\right],
\end{aligned} \tag{8}$$

where $\beta = \sqrt{k^2 - \gamma^2}$, $\beta_s = \sqrt{\varepsilon_s k^2 - \gamma^2}$, $\beta_f = \sqrt{\varepsilon_f k^2 - \gamma^2}$ are transverse wave numbers in the air, substrate and film media respectively, d_s is substrate thickness, d_f is film thickness, a is width of wide wall of waveguide, γ is propagation constant, k is free space wave number. In this equation, the position of film-substrate boundary assumed to be exactly at the middle of waveguide, however known displacement can be taken in account.

3.3 Experimental result

Described measurement technique was utilized for study of BST thin films. The film of about 1 μm thickness was deposited onto 0.5mm MgO substrate in a pulsed laser ablation setup. Special measurement cell was elaborated to provide reliable contact of specimen under test with waveguide walls, Fig. 14. Automatic network analyzer was calibrated with

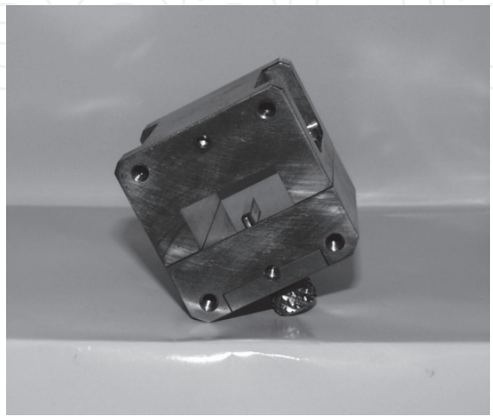

Fig. 14. Waveguide measurement cell for thin films study

appropriate X-band calibration kit. Then two reference measurements were performed. First one is a measurement of empty cell. It makes possible to determine cell's electrical length more precisely. Second one is the measuring of substrate alone. This stage is required to determine the actual loss of the "substrate-in-waveguide" system because only on this background film properties will be recognized.
Numerous experiments with the same samples show reliable repeatability of experiments. Fig. 15 illustrates an example of measured data fitting for MgO substrate and 0.84μm thick BST film.

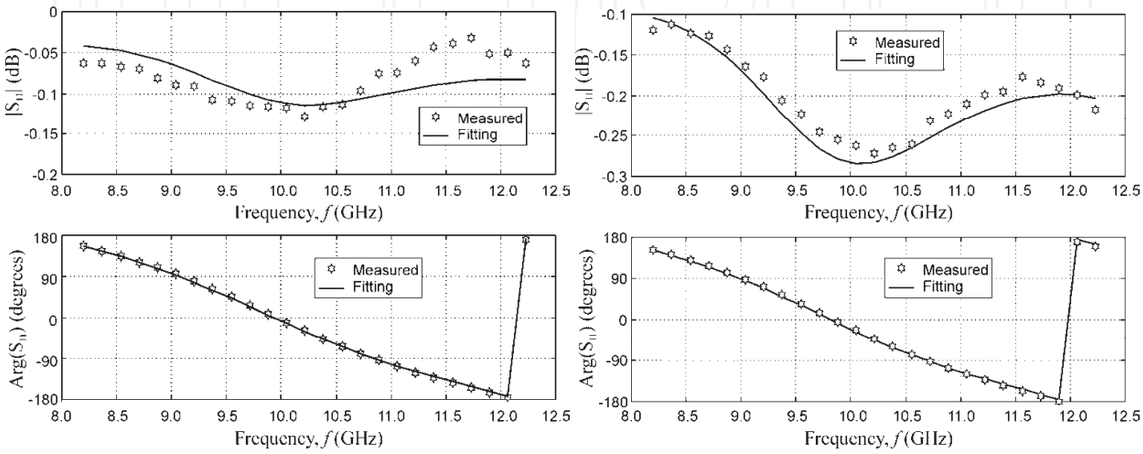

Fig. 15. Measured data and calculation for: 0.5 mm thickness MgO substrate (*a*), 0.84 μm BST film on 0.5 mm thickness MgO substrate. Specimen dimensions are 22 × 10 mm (*b*)

Average value of substrate permittivity is ε′ = 9.9, tanδ = $3 \cdot 10^{-4}$. As to the film fitting to the calculation exhibits good agreement and yields ε = 450, tanδ = 0.05. Both reflection of shorted waveguide with sample and transmission in the 2-port system can be used, however the first method is preferable because of higher sensitivity.
Presented technique of thin ferroelectric film examination can be applied also for study of relatively thick (10μm and more) films that have non-ferroelectric nature. The method can be successfully used, for example, to study semiconductor films deposited onto dielectric subtract when traditional metering technique brakes down.

3.4 Uncertainty of non-resonant waveguide method for thin films measurement

Ideal contact of studied specimen with waveguide walls is hard to achieve and there small air gaps on the interface. These gaps may degrade accuracy substantially. Though some estimations consider 2.5-7 μm gap acceptable (Champlin & Glover, 1966), this value is too general and hard to verify. So it is desirable to enforce interface contact as much as possible.
Though films permittivity and loss are estimated using least squares curve fitting technique (3), let's begin uncertainty estimation with single point accuracy. Parameters of studied film are derived from indirect measurements. They contain uncertainties of dimensions measurements, scattering parameters magnitude and phase uncertainties, and rounding errors of processing procedure. In waveguide experiment magnitude and phase of reflection coefficient are measured directly (real and imaginary part to be precise, but that does not change further explanations). Their simulation values depend on sample's physical dimensions, permittivity and loss:

$$\dot{S} = \dot{S}\left(\varepsilon_f, \tan\delta_f, \varepsilon_s, \tan\delta_s, L, d_f, d_s\right), \tag{9}$$

where $\varepsilon_f, \tan\delta_f$ is permittivity and loss of studied film, $\varepsilon_s, \tan\delta_s$ is permittivity and loss of the substrate, L is sample's length, d_f, d_s is film and substrate thickness respectively. This equation is implicit function, which relates mentioned parameters.

Due to low loss substrate effective loss of measurement cell is low. In such conditions permittivity is mainly found by phase measurement, whereas loss is found from magnitude measurements (Janezic & Jargon, 1999). Large difference in sensitivities allows separate analysis of permittivity and loss uncertainties.

Sensitivities of calculated values of film's permittivity and loss to uncertainties of directly measured values can be estimated using rules of implicit function differentiation. Then for every given frequency permittivity and loss uncertainty can be expressed as:

$$\begin{aligned}
\Delta\varepsilon_f &= \frac{1}{\dfrac{\partial\angle S_{11}}{\partial\varepsilon_f}}\sqrt{\left(\frac{\partial\angle S_{11}}{\partial L}\Delta L\right)^2 + \left(\frac{\partial\angle S_{11}}{\partial d_f}\Delta d_f\right)^2 + \left(\Delta\angle S_{11}\right)^2 + \left(\frac{\partial\angle S_{11}}{\partial\varepsilon_s}\Delta\varepsilon_s\right)^2}; \\
\Delta\tan\delta_f &= \frac{1}{\dfrac{\partial|S_{11}|}{\partial\tan\delta_f}}\sqrt{\left(\frac{\partial|S_{11}|}{\partial L}\Delta L\right)^2 + \left(\frac{\partial|S_{11}|}{\partial d_f}\Delta d_f\right)^2 + \left(\Delta|S_{11}|\right)^2 + \left(\frac{\partial|S_{11}|}{\partial\tan\delta_s}\Delta\tan\delta_s\right)^2},
\end{aligned} \tag{10}$$

where ΔL uncertainty of length measurement, Δd_f is uncertainty of film thickness measurement, $\Delta|S_{11}|$ is uncertainty of magnitude of scattering parameter, $\Delta\angle S$ is uncertainty of phase of scattering parameter, $\Delta\varepsilon_s$ and $\Delta\tan\delta_s$ is uncertainty of substrate's parameters. Listed uncertainties are related to instrument uncertainties. Uncertainty of substrate thickness measurement is usually much smaller, than listed values, so it is omitted for the sake of clarity, though might be accounted exactly same way. Listed uncertainties were estimated numerically for the following conditions: frequency 10 GHz, film's thickness 1 μm, film's permittivity ε = 500, loss tanδ = 0.05, sample length 20 mm, substrate thickness 0.5 mm, permittivity ε = 9.9, loss tanδ = 10^{-4}, their values presented in Table 3. Table 4 presents summary on instrument uncertainties.

$\frac{\partial\angle S_{11}}{\partial\varepsilon_f}, \frac{\text{deg}}{}$	$\frac{\partial\angle S_{11}}{\partial L}, \frac{\text{deg}}{m}$	$\frac{\partial\angle S_{11}}{\partial d_f}, \frac{\text{deg}}{m}$	$\frac{\partial\angle S_{11}}{\partial\varepsilon_s}, \frac{\text{deg}}{}$
0.04	35000	$2.2\cdot10^7$	22
$\frac{\partial\lvert S_{11}\rvert}{\partial L}, \frac{dB}{m}$	$\frac{\partial\lvert S_{11}\rvert}{\partial d_f}, \frac{dB}{m}$	$\frac{\partial\lvert S_{11}\rvert}{\partial\tan\delta_s}, \frac{dB}{}$	$\frac{\partial\lvert S_{11}\rvert}{\partial\tan\delta_f}, \frac{dB}{}$
30	1700	0.02	4.23

Table 3. Sensitivities to uncertainties of directly measured values

Parameter	Value	Note
ΔL	10 μm	Micrometre screw
Δd_f	10 nm	Reflectometer
$\Delta\varepsilon_s$	0.1	1%
$\Delta\tan\delta_s$	10^{-4}	10%
$\Delta\lvert S_{11}\rvert$	0.02	HP 8510C
$\Delta\angle S_{11}$	2°	HP 8510C

Table 4. Instrument uncertainties

For the film under consideration uncertainty of permittivity measurement $\Delta\varepsilon/\varepsilon$ is about 14%, while uncertainty of loss measurement $\Delta\tan\delta_f/\tan\delta$ is about 93%. For the film with loss $\tan\delta = 0.1$ loss uncertainty will be 47%.
If method applied for film study in production process, i.e. the same substrate used in all measurements, then uncertainty of substrate permittivity and loss could be eliminated and permittivity uncertainty improves to about 10%.
These values present worst case estimation of single point measurement. Uncertainty of final parameters is reduced by least squares processing. With 50 point equally distributed along measurement frequency range sensitivity to uncertainty of scattering parameter determination can be reduced by order of magnitude to

$$\frac{\partial\varepsilon_f}{\partial\angle S_{11}} = 3\frac{1}{\text{deg}}; \qquad \frac{\partial\tan\delta_f}{\partial\lvert S_{11}\rvert} = 0.15.$$

Then averaged uncertainty of film's permittivity reduces to 2% and loss to 10%.

3.5 Coplanar line method

In actual devices a system of electrodes is deposited on the surface of ferroelectric film. Geometry of the electrodes depends on film permittivity. At the same time metal electrodes can modify film permittivity and loss. Therefore it would be desirable to perform measurement directly in the device with deposited electrodes.
One of the most usable electrode system forms a coplanar line, Fig.16. Measurement of permittivity and loss of ferroelectric film integrated in coplanar line is discussed below.

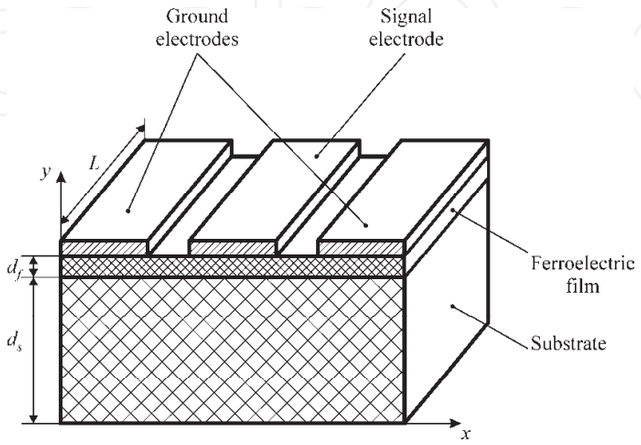

Fig. 16. Coplanar line on substrate with deposited ferroelectric film

Electromagnetic field problem for the structure given in Fig.16 was solved by finite element method. Electromagnetic field of quasi TEM mode was described in terms of vector and scalar potential applying the Lorenz gauge. As a result the problem was reduced to partial differential equation for scalar potential φ :

$$\nabla\left(\varepsilon(y)\nabla\varphi\right)+\varepsilon^2(y)k^2\varphi=0\,, \tag{11}$$

where $\varepsilon(y)$ is distribution of dielectric permittivity along the y – axis. Characteristic impedance Z and effective permittivity ε_{ef} of coplanar line can be found from solution of equation (11) by formulas:

$$Z=Z_0\frac{V^2}{\sum\limits_{i=1}^{N}\sqrt{\varepsilon_i}\iint\limits_{S_i}\left(\left(\frac{\partial\varphi}{\partial x}\right)^2+\left(\frac{\partial\varphi}{\partial y}\right)^2\right)dxdy};$$
$$\varepsilon_{ef}=\frac{\sum\limits_{i=1}^{N}\left(\varepsilon_i\iint\limits_{S_i}\left(\left(\frac{\partial\varphi}{\partial x}\right)^2+\left(\frac{\partial\varphi}{\partial y}\right)^2\right)dxdy\right)}{\iint\limits_{S}\left(\left(\frac{\partial\varphi_1}{\partial x}\right)^2+\left(\frac{\partial\varphi_1}{\partial y}\right)^2\right)dxdy}, \tag{12}$$

where $Z_0\approx 120\pi\ \Omega$ is the characteristic impedance of free space, V is the electrode voltage, N is the quantity of domains with different permittivities, ε_i is the permittivity of the i -th domain, S_i is the cross-section are of the i -th domain, φ_1 is the solution of the equation (11) for the case if $\varepsilon_i=1, i=\overline{1,N}$.

Dependences of characteristic impedance and effective permittivity of coplanar line deposited on the ferroelectric film and low permittivity dielectric wafer versus permittivity of ferroelectric film and its thickness are shown in Fig.17.

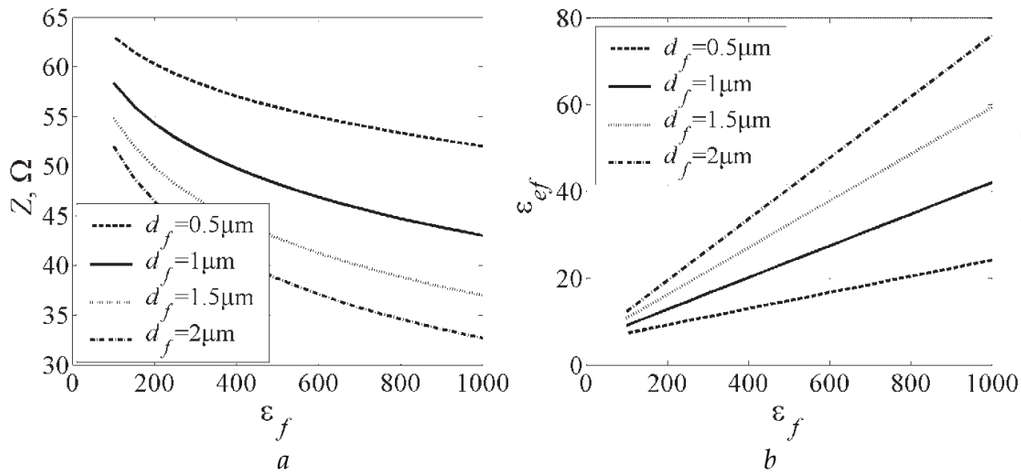

Fig. 17. Characteristic impedance (a) and effective permittivity (b) of coplanar line versus permittivity and thickness of ferroelectric film deposited on substrate with permittivity equal to 10

Measurement cell for study of permittivity and loss tangent of ferroelectric film is shown in Fig.18. Two-port measurement of frequency dependences of scattering parameters was performed by vector network analyzer.

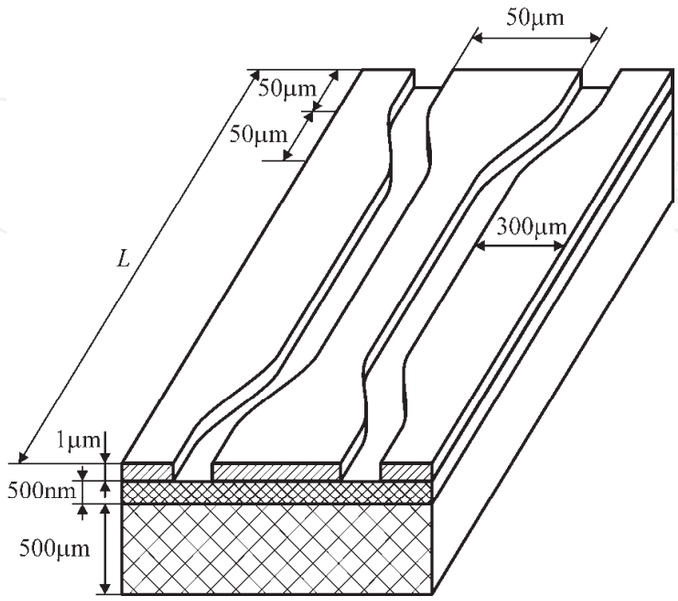

Fig. 18. Coplanar line measurement cell

Scattering matrix of coplanar line section with the length equal to L connected to ports with characteristic impedance Z_1 can be calculated from formulas:

$$S_{11} = j\frac{\left(Z^2 - Z_1^2\right)\sin\left(\gamma L\right)}{2ZZ_1\cos\left(\gamma L\right) + j\left(Z^2 + Z_1^2\right)\sin\left(\gamma L\right)}, \tag{13}$$

$$S_{21} = \frac{2ZZ_1}{2ZZ_1\cos\left(\gamma L\right) + j\left(Z^2 + Z_1^2\right)\sin\left(\gamma L\right)}, \tag{14}$$

where $\gamma = \dfrac{2\pi f\sqrt{\varepsilon_{ef}}}{c}$ is the propagation constant in the coplanar line.

Measured frequency dependences of scattering matrix parameters were approximated by formulas (13) and (14) by least square method:

$$\min_{\left(\varepsilon_f,\,\tan\delta_f\right)}\sum_n \sigma_n\left(S_n^{meas} - S\left(f_n,\varepsilon_f,\tan\delta_f\right)\right)^2, \tag{15}$$

where $S\left(f_n,\varepsilon_f,\tan\delta_f\right)$ is calculated value of scattering parameter at the frequency f_n assuming tested film to have permittivity ε_f and loss tangent $\tan\delta_f$.

Fig.19 demonstrates measured and calculated after solving of approximation problem (15) the frequency dependences of scattering matrix parameters for the structure presented in Fig.18.

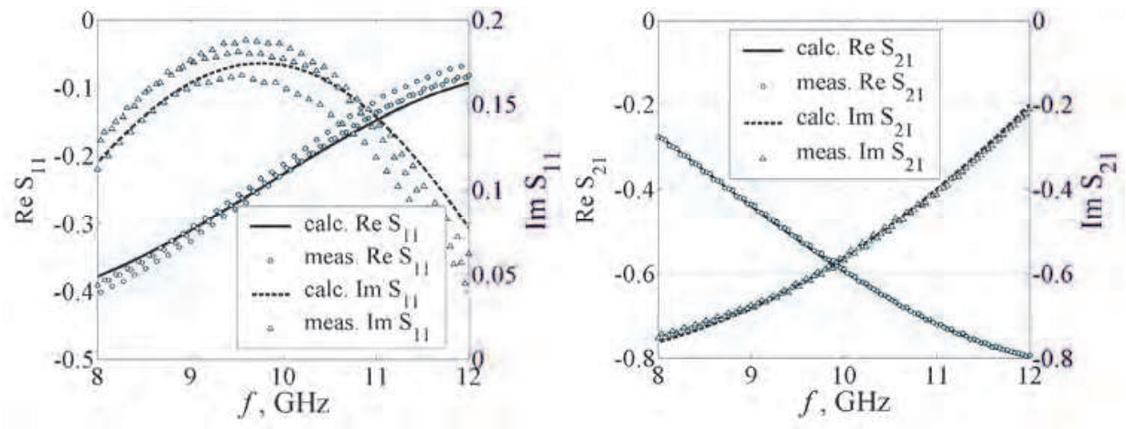

a b

Fig. 19. Measured and calculated frequency dependences of scattering matrix parameters S_{11} (a) and S_{21} for the structure shown in Fig. 18

Relative uncertainty of film permittivity measurement can be defined as uncertainty of implicit measurement:

$$\delta\varepsilon_f = \frac{1}{\left|\Theta^S_{\varepsilon_f}\right|}\sqrt{(\delta \mathrm{S})^2 + \left(\Theta^S_{d_f}\delta d_f\right)^2 + \left(\Theta^S_L \delta L\right)^2 + \left(\Theta^S_h \delta h\right)^2 + \left(\Theta^S_{\varepsilon_s}\delta\varepsilon_\mathrm{s}\right)^2} \tag{16}$$

where $\Theta^\alpha_\beta = \frac{\beta}{\alpha}\frac{\partial\alpha}{\partial\beta}$ is the sensitivity of the parameter α to alteration of the parameter β, $\delta\beta$ is the relative uncertainty of the parameter β measurement, S is the measured parameter of scattering matrix, ε_s is the permittivity of substrate, h is the substrate thickness.

Analysis of the formula (16) predicts that uncertainty of film thickness measurement makes the main contribution in measurement uncertainty of film permittivity. Estimation prediction of film permittivity measurement uncertainty is about 10% if uncertainty of film thickness measurement is about 10 nm for the film thickness about 500 nm and its permittivity around 200. The uncertainty rises up while either film thickness or its permittivity decreases.

Uncertainty of film loss tangent measurement is larger than uncertainty of permittivity measurement because of smaller value of the sensitivity of scattering matrix parameters to alteration of film loss tangent $\Theta^S_{\tan\delta_f}$. Estimation predicts the uncertainty of film loss tangent measurement around 30% for the film thickness about 500 nm and its permittivity around 200.

Described technique was verified during measurement of ferroelectric films deposited by sol-gel method on semi-insulated silicon substrate. Some results of the verification are presented in table 5.

Ferroelectric film composition	Annealing temperature, °C	Film thickness, μm	Permittivity
$Pb(Ti,Zr)O_3$	700	0.35	90±15
$Pb(Ti,Zr)O_3$	800	0.35	120±15
$(Ba,Sr)TiO_3$	650	0.2	125±30
$(Ba,Sr)TiO_3$	750	0.2	250±40

Table 5. Results of investigation of ferroelectric films deposited on semi-insulated silicon substrate by sol-gel method

3.6 Resonator method description

Thin ferroelectric films can also be studied using composite dielectric resonator (CDR) method. Simple equations for effective permittivity and loss, based on parallel layers model, in case of significant difference in layers thickness, which is a case for thin films, give inadequate results. Thus, electromagnetic problem for "film-on-substrate" composite dielectric resonator should be solved without approximations.

To calculate resonant frequencies of the CDR one may solve electromagnetic problem for the configuration, depicted in Fig. 20. Square shaped CDR of length L and thickness d_s is made from material with ε_s and placed inside waveguide with $a \times b$ cross-section parallel to its narrow wall. Waveguide is filled with ε_a. Dielectric film of thickness d_f and permittivity ε_f is deposited onto resonator surface. The problem is solved using partial domains method.

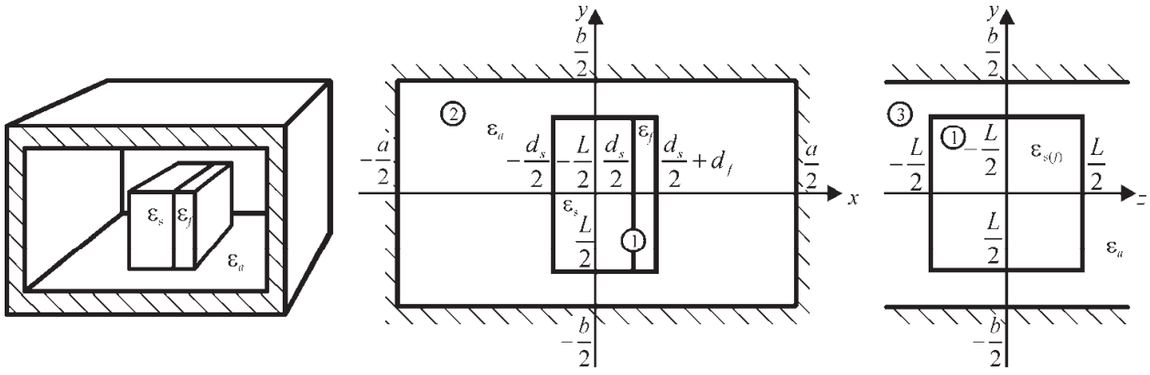

Fig. 20. Square shape CDR with film inside of rectangular waveguide

In every domain 1 and 2 electromagnetic field may be expressed using x-components of electrical $\Gamma^e = (\Gamma^e,0,0)$ and magnetic $\Gamma^m = (\Gamma^m,0,0)$ Hertz vectors. To do that electromagnetic field in every domain is presented as series of eigen functions:

$$\Gamma_i^{e(m)} = \sum_{j=0}^{\infty} A_{ij}^{e(m)} \Phi_{ij}^{e(m)}(x,y) Z_{ij}^{e(m)}(z), \tag{17}$$

where i is number of partial domain, $A_{ij}^{e(m)}$ series coefficients to be found, $\Phi_{ij}^{e(m)}(x,y)$ is eigen function number j of partial domain number i,, $Z_{ij}^{e(m)}(z)$ is solution of Helmholtz equation in every domain.

Using equality requirement for tangential components of the field in $|z|=\frac{L}{2}$ planes the problem can be reduced to the set of homogenous Fredholm's integral equations of the I kind relative to distribution of magnetic and electric Hertz vectors $\Psi^e(x,y)$, $\Psi^m(x,y)$:

$$\iint_S \left(G_n^e(x,x',y,y')\Psi^e(x,y)+G_n^m(x,x',y,y')\Psi^m(x,y)\right)dxdy=0,\quad n=1,2, \tag{18}$$

where S is waveguide cross-section. Integral equations kernels $G_n^e(x,x',y,y')$, $G_n^m(x,x',y,y')$ can be expressed with eigen functions of areas $\Phi_{ij}^{e(m)}(x,y)$, $Z_{ij}^{e(m)}(z)$ and their derivatives. Integral equation can be solved using the method of moments, so finally electromagnetic problem reduces to nonlinear eigen values problem. These eigen values are the resonant frequencies of studied system.

Basic mode oscillations can be excited as in waveguide, so in resonator itself. However, in matched waveguide section there are no parasitic oscillations, which are natural to standalone resonator.

CDR's made of Al_2O_3 (ε =9.6), $BaTi_4O_9$, and $DyScO_3$, $SmScO_3$, LSAT with ε = 26.3, 25.1, 22.7 respectively were simulated and studied experimentally. CDR dimensions ratio was in the range d/L = 0.2…0.01. Results summary is presented in Fig. 21.

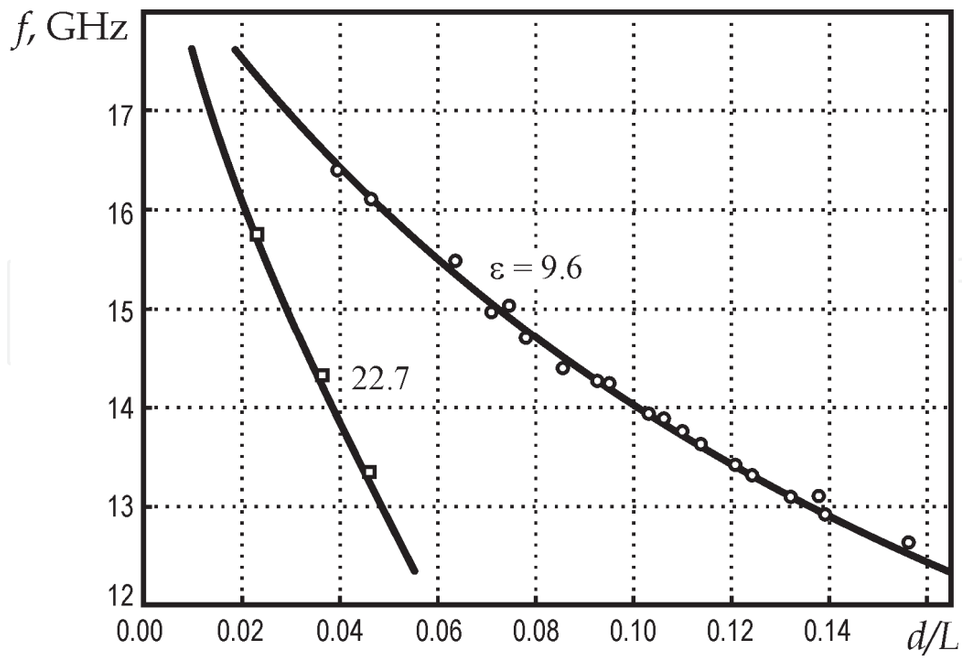

Fig. 21. Simulated and measured dependencies of CDR resonant frequency for small dimensions ratio (d/L) with ε_s = 9.6, 22.7, 26.3

Because all measurements are held relative resonant frequency of resonator without film, uncertainty depends mainly on dimensions uncertainty. Resonant frequency shift for CDR with film depends on film's thickness, Fig. 22. Frequency range, where this method is applicable, depends on CDR's resonant frequencies, which in turn depend on dimensions and substrate permittivity.

To reduce measurement uncertainty the resonator thickness d_s should be rather small. However it leads to increasing of resonator length L which would be greater than narrow wall width. In this case the resonator should be placed by such a way that ferroelectric film surface would be almost parallel to wide wall of waveguide with some angle shift to satisfy resonator excitation condition.

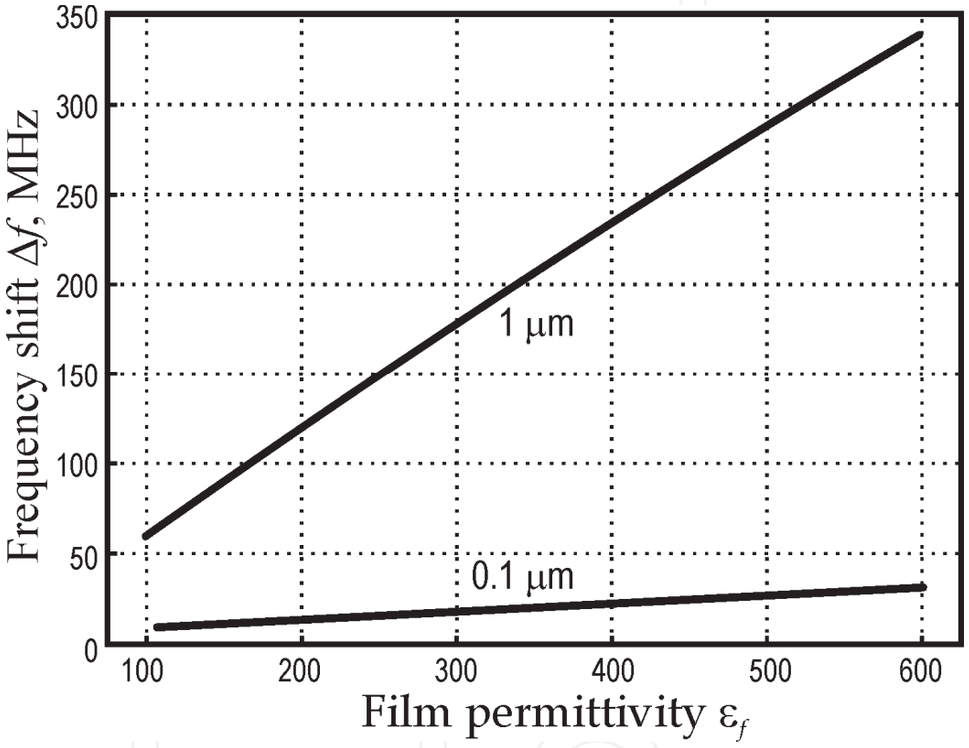

Fig. 22. Resonant frequency shift for 1 μm and 0.1 μm films on 0.1 mm thick substrate with ε = 26

4. Conclusion

Electrodeless methods for bulk and thin film ferroelectric materials study presented. In non-resonant methods partial filling of waveguide cross-section may be applied for rare and expensive materials study. Permittivity and loss of studied specimen are determined by solving scattering equations for waveguide section with studied specimen against measured scattering parameters. The choice for transmission or reflection method depends on sensitivity of scattering matrix to change of ε and tanδ of studied specimen. Study of scattering parameters frequency dependency and subsequent their approximation with appropriate measurement cell models allows to increase measurement accuracy and reduce susceptibility to random error.

To measure ε and tanδ of thin films studied specimen may be located lengthwise inside of rectangular waveguide. This allows better interaction of thin film with electromagnetic field.

For the system with metal electrodes deposited on the surface of ferroelectric film the coplanar line technique may be applied. This method can be extended for other electrode layouts.

Another option for thin films study might be use of resonant techniques. To increase sensitivity to film's properties thin composite resonator required. However, to tune it to required frequency composite resonator should have larger dimensions, thus irregular waveguide might be required. Otherwise sample should be oriented with large tilt angle, almost normal to waveguide's wide wall.

5. References

Baker-Jarvis J. (1990). Transmission/reflection and short-circuit line permittivity measurements, *NIST Technical Note 1341*, Jul. 1990

Baker-Jarvis, J. Geyer, R. G. & Domich, P. D. (1992). A nonlinear least-squares solution with causality constraints applied to transmission line permittivity and permeability determination. *IEEE Trans. on Instr. and Meas.,* Vol: 41, Issue: 5, Oct. 1992, pp. 646 – 652.

Balanis, C. A. (1989). *Advanced Engineering Electromagnetics*, Wiley, 1989, pp. 394–409, ISBN 0-471-62194-3

Banieki, J. D.; Laibowitz, R. R.; Shaw, T. M.; Duncombe, P. R. & Neumayer, D. A. (1998). Dielectric relaxation of Ba0.7Sr0.3TiO3 films from 1 MHz to 20 GHz, *Applied Phys. Lett.*, vol. 72, pp. 498-500, 1998

Champlin, K. S. & Glover, G. H. (1966). Gap effect in measurements of large permittivity. *IEEE Trans. Microwave Theory Tech.*, 1966, vol. 14, pp. 397-398

Egorov, Y. V. (1967). *Partially filled rectangular waveguides*, Soviet radio, Moscow, 1967, pp. 19–72 (in Russian).

Erker, E. G.; Nagra, A. S.; Liu, Yu; Periaswami, P.; Taylor, T. R.; Speck, J. & York, R.A. (2000). Monolitic Ka-band phase shifter using voltage tunable BaStTiO3 parallel plate capacitors. *IEEE Microwave and Guided Wave Letters*, vol. 10, # 1, January 2000, pp. 7-12

Gevorgian, S. S. & Kollberg, E.L. (2001). Do we really need ferroelectrics in paraelectric phase only in electrically controlled microwave devices? *IEEE Trans. Microwave Theory Tech.*, vol. 49, #11, Nov. 2001, pp.2117-2123

Janezic, M. D. & Jargon, J. A. (1999). Complex permittivity determination from propagation constant measurements. *IEEE Microwave and Guided Wave Letters*. Vol. 9, Issue 2, Feb. 1999, P. 76 – 78

Lanagan, M. T.; Kim, J. H.; Dube, D. C.; Jang, S. J. & Newnham, R. E. (1988). A Microwave Dielectric Measurement Technique for High Permittivity Materials, *Ferroelectrics*, Vol. 82, 1988, pp. 91-97

Vendik, O. G. (Ed.). (1979). *Ferroelectrics at Microwaves*, Soviet Radio, Moscow, Russia (in Russian)

Vendik, O. G.; Vendik, I. B. & Samoilova, T. B. (1999). Nonlinearity of superconducting transmission line and microstrip resonator. *IEEE Trans. Microwave Theory Tech.*, vol. 45, #2, Feb. 1999, pp. 173-178

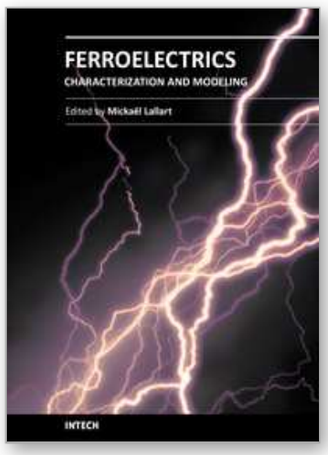

Ferroelectrics - Characterization and Modeling

Edited by Dr. MickaÃ«l Lallart

ISBN 978-953-307-455-9
Hard cover, 586 pages
Publisher InTech
Published online 23, August, 2011
Published in print edition August, 2011

Ferroelectric materials have been and still are widely used in many applications, that have moved from sonar towards breakthrough technologies such as memories or optical devices. This book is a part of a four volume collection (covering material aspects, physical effects, characterization and modeling, and applications) and focuses on the characterization of ferroelectric materials, including structural, electrical and multiphysic aspects, as well as innovative techniques for modeling and predicting the performance of these devices using phenomenological approaches and nonlinear methods. Hence, the aim of this book is to provide an up-to-date review of recent scientific findings and recent advances in the field of ferroelectric system characterization and modeling, allowing a deep understanding of ferroelectricity.

INTECH
open science | open minds

InTech Europe
University Campus STeP Ri
Slavka Krautzeka 83/A
51000 Rijeka, Croatia
Phone: +385 (51) 770 447
Fax: +385 (51) 686 166
www.intechopen.com

InTech China
Unit 405, Office Block, Hotel Equatorial Shanghai
No.65, Yan An Road (West), Shanghai, 200040, China
中国上海市延安西路65号上海国际贵都大饭店办公楼405单元
Phone: +86-21-62489820
Fax: +86-21-62489821

IntechOpen